RSC Advances

PAPER

View Article Online
View Journal | View Issue

Cite this: *RSC Adv.*, 2020, **10**, 8008

Superhydrophobic paper with mussel-inspired polydimethylsiloxane–silica nanoparticle coatings for effective oil/water separation

Xuewei Ruan, *[ab] Tiancheng Xu,[b] Dingjiang Chen,[a] Ziwen Ruan[b] and Haitu Hu[b]

Received 2nd October 2019
Accepted 19th January 2020

DOI: 10.1039/c9ra08018j

rsc.li/rsc-advances

Although various filtration materials with (super)wetting properties have been fabricated for effective oil/water separation, eco-friendly and low-cost materials are still highly desired. This work details the facile preparation of efficient oil–water separation papers with superhydrophobic properties that successfully combine micro/nanoscale hierarchical particles and low surface energy components with porous substrates. The superhydrophilic papers were coated with a polydopamine layer and then immersed in the mixture of polydimethylsiloxane (PDMS) and hydrophobic-silica nanoparticles. The resultant paper can separate oil–water mixtures under gravity driving conditions, where heavy oil penetrates through the sample and water is collected on the surface. And the as-prepared sample had favorable separation efficiency (>99%). More importantly, the oil flux almost remained at the original value after 10 cycles, indicating excellent recyclability. In addition, the as-prepared paper exhibits good stability in acidic, alkaline and salty media.

Introduction

Effective separation for oil–water has drawn significant worldwide attention because of the weaknesses in freshwater supply for the rapidly growing global human population. This kind of wastewater comes from a variety of sources such as crude oil production and refineries, petrochemical, pharmaceutical, metal processing, and textile production industries, and oil spill accidents from storage tanks or transport facilities. They often contain various toxic substances such as phenols, petroleum hydrocarbons, polyaromatic hydrocarbons, metal ions, and radioactive elements that possess mutagenic and carcinogenic risks to plants, animals and human beings.[1–3] A variety of conventional methods such as gravity or density separation, burning, skimming, centrifugation, coagulation, adsorption, *etc.*, have been invented to separate oil–water.[4–11] However, these methods are not completely satisfactory. For instance, the coagulation and gravity separation techniques are low efficiency and multistage (Fig. 1A).

Recently, filtration techniques have been proved to be one of the best methods for effective separation of oil–water, which only allows a selected phase (either oil or water) to penetrate, while preventing the other phase from passing through. Various polymer membranes,[12–16] metal meshes,[17–20] nanofibers,[21,22] graphene oxide/carbon nanotube filters[23–26] with selective wettability have been fabricated *via* phase separation, electrochemical deposition, chemical vapor deposition, dip coating, *etc.* Now, superhydrophobic/superoleophilic "oil-removing" materials and underwater superoleophobic "water removing" materials have received a great deal of attention. Hydrophobic polydimethylsiloxane (PDMS) is one of the most important materials in the preparation of superhydrophobic and superoleophobic surfaces based on its very low surface tension and self-roughening.[27–32]

Dopamine, the most renowned catecholamine, is able to undergo self-polymerization under oxidizing conditions, creating a bioinspired surface-adherent polydopamine (PDA) coating on almost all kinds of organic and inorganic surfaces.[33–36] Moreover, PDA chains incorporate many functional groups such as catechol, amine, and imine, that can serve as the reactive sites with desired molecules and the anchors for the loading of transition metal ions *via* bidentate coordination, hydrogen bonding, Michael addition or Schiff base reactions for efficient oil/water separation.[34,37–42] Lee group modified anodic aluminum oxide (AAO) membranes by adhesion mechanisms of PDA and soft-lithographic technique. The modified superhydrophobic surface showed high-water adhesion properties, that can be used as a water-capturing device shown in the cuticle of the Namib desert beetle.[43] Xie group prepared a stable three-dimensional composite sponge with magnetic by situ coating of dopamine and followed by immersing in the mixture of magnetic Fe_3O_4 nanoparticles and PDMS. The modified sponge exhibited high adsorption capacity for diverse organic solvents and can be easily recovered in oil–water mixture under magnetism.[44]

[a]*College of Environmental and Resource Sciences, Zhejiang University, Hangzhou, 310027, P. R. China. E-mail: xuewei.r@outlook.com*

[b]*Zhejiang Baocheng Machine Science Technology Co., Ltd, Ningbo, 315033, P. R. China*

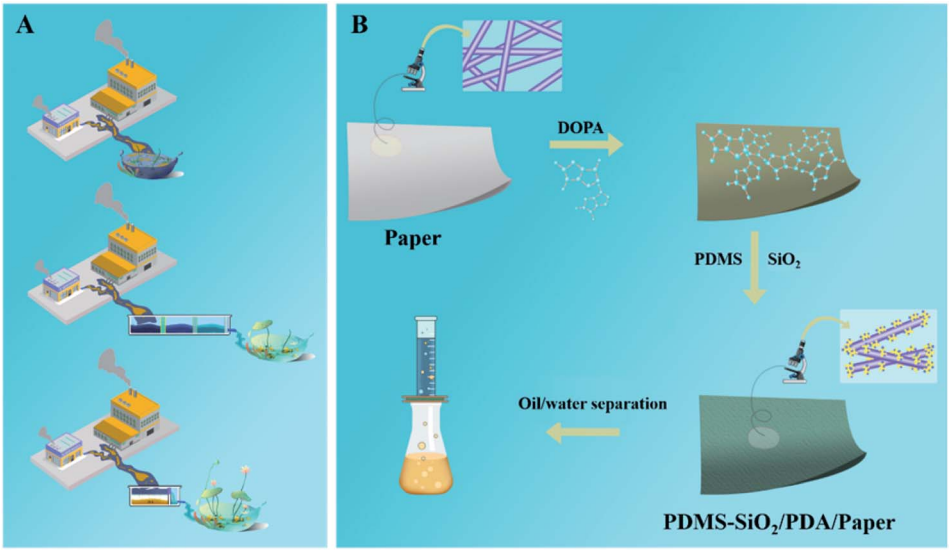

Fig. 1 Schematic illustration of oil/water separation processes by the coagulation and gravity separation techniques (A) and the fabrication for the film of PDMS–SiO_2/PDA/paper and its application for oil/water separation (B).

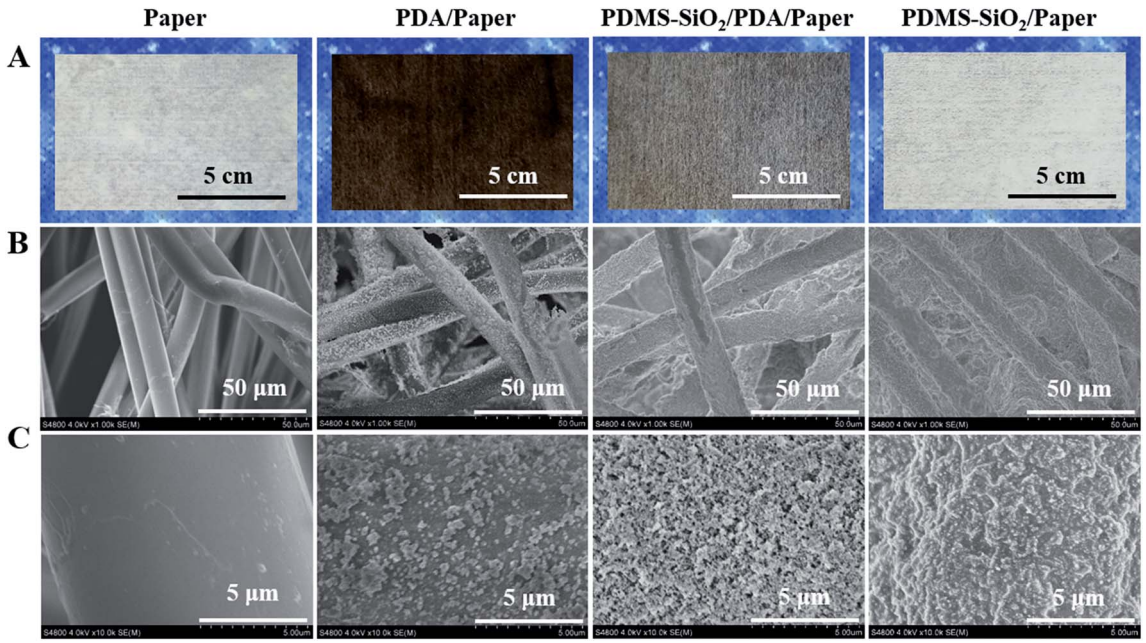

Fig. 2 (A) Photographs, (B and C) SEM images of the papers before and after mussel-inspired surface coating.

However, the (super)wetting materials for effective oil–water separation are confined to some extents due to the inevitable rapid consumption of non-renewable and their high-cost. Additionally, the polluted separation materials are directly discarded or burnt, inevitably leading to the secondary pollution to the environment, although the oil pollution problem has been solved. Therefore, it is very important to develop eco-friendly and low-cost green materials for oil/water separation. In this work, environmentally friendly and abundant tissue paper with hydrophobicity is developed by coating of dopamine and followed by immersing in the mixed suspension of PDMS and SiO_2 nanoparticles. The as-prepared PDMS–SiO_2/PDA/paper exhibits high porosity, strong water repellence, low water-adhesion force, and excellent mechanical strength. Moreover, the highly efficiency and large flux for treating multiple type oil–water mixtures was achieved, and the separation mechanism was investigated in detail.

Experimental

Materials and reagents

Tissue papers were bought from Tmall, China. Polydimethylsiloxane (PDMS) precursor and curing agent (Sylgard 184) were purchased from Dow Corning. Nano fumed silica

(SiO_2, hydrophobic-260, 7–40 nm), dopamine (DA), tris(hydroxymethyl)aminomethane hydrochloride (Tris), ethyl acetate, trichloromethane, carbon tetrachloride, 1,2-dichloroethane, red oil O and methylene blue were used directly and purchased from Aladdin, China. Sodium chloride (NaCl), hydrochloric acid, ethanol and sodium hydroxide were supplied by Sinopharm Chemical Reagent Co.

Fabrication of hydrophobic tissue paper

PDMS–SiO_2/PDA/paper films were fabricated by mussel-inspired surface coating technique as shown in Fig. 1B. In a typical synthesis, the tissue papers were first immersed in 5 g L^{-1} DA solution in Tris–HCl buffer solution (pH 8.5, 10 mM) at 40 °C for 12 h under continuous shaking. Then they were taken out, washed thoroughly in water, and dried under vacuum. The sample was named as PDA/paper. The coating yield of PDA on paper was 13.1 ± 0.5 wt%, which was calculated by measuring the weights of the paper before and after surface coating. Nano-SiO_2 (1 wt%) was dispersed in the solution of PDMS precursor (4 wt%) and curing agent (0.4 wt%) in ethyl acetate under stirring for 30 min at room temperature, then the mixture was sonicated for 30 min to ensure the homo-dispersion of nanoparticles. Subsequently, the obtained PDA/paper samples were soaked in the mixture for 1 min. They were taken out, washed with water and dried at 80 °C for 4 h and named as PDMS–SiO_2/PDA/paper. The coating yield of PDMS–SiO_2 on PDA/paper was 22.7 ± 0.9 wt%. As a control, PDMS–SiO_2 modified paper (PDMS–SiO_2/paper) was fabricated by the same procedures. The coating yield of PDMS–SiO_2 on paper was 28.6 ± 1.1 wt%.

Characterization

The morphologies and the elemental analysis of the samples were characterized by a field-emission scanning electron microscope (FESEM, Hitachi S-4800, Japan) equipped with an X-ray energy dispersive spectroscopy (EDS). Fourier transform infrared spectrometer (ATR-FTIR, Thermo-Nicolet 6700, USA) was used to characterize chemical composition of the papers. Tensile strength and elongation at break of the samples with a size of 20 mm × 10 mm (length × width) were measured by a tensile tester (Instron 5567, US) at a speed of 10 mm min^{-1}. Membrane porosity (%) was characterized by dry-humid weight method using 1-butanol as the testing liquid and calculated according to eqn (1):

$$\text{Porosity} = \frac{(m_w - m_d)/\rho_1}{(m_w - m_d)/\rho_1 + m_d/\rho_2} \times 100 \quad (1)$$

where m_d (g) and m_w (g) refers to the mass of the samples before and after immersing in 1-butanol respectively, ρ_1 (g cm^{-3}) and ρ_2 (g cm^{-3}) is the density of 1-butanol and the paper.

Contact angle (CA) of the samples was conducted using an OCA20 machine (Data Physics, Germany) equipped with a video capture at ambient temperature. The adopted CA was the average value of at least five measurements performed at different positions on the same sample. The water-adhesion force was measured using a high-sensitivity micro-electromechanical balance system (Data-Physics DCAT11, Germany). A water droplet (5 μL) was suspended with a metal cap, then the sample moved upward at a constant speed of 0.5 mm s^{-1} until touching the droplet, then keeps moving upward for 0.2 mm. At last, the sample moved downward to the initial position, and the distance–force curve was recorded. The impact process of a water droplet on the sample surface was recorded by a camera (FASTCAM Mini UX100, Photron Limited, Japan) at a rate of 1000 frames per second.

Oil/water separation of the sample was characterized by a dead-end filtration cell with an effective diameter of 2.5 cm gravity driving conditions. The sample was sealed between one vertical glass tube and one conical flask. 15 mL oil colored by oil red O and 15 mL water colored by methyl blue was poured in the cell, oil or water spontaneously permeated quickly. The flux (J, L m^{-2} h^{-1}) was calculated according to eqn (2). The separation efficiency (SE, %) of the samples was characterized by the residual oil content in the water after permeation of the mixture through the sample. The oil concentration in water after separation was measured by an infrared photometer oil content analyzer (Beijing Fly Seth Technology Co., LTD, OL680). To evaluate the reusability of the samples, the sample was washed with acetone for 5 min after a solvent separation, then the next oil–water separation experiment was carried out again.

$$J = \frac{V}{At} \quad (2)$$

where V (L) represents the permeated volume, A (m^2) represents the effective area of the sample, and t (h) is the operation time.

To characterize the liquid absorption capacity, a piece of sample was immersed in oil or water for 10 min, left on a metal net and wiped quickly to remove the excess liquid. The liquid absorption capacity (C) was calculated according to eqn (3), where m_1 (g) and m_2 (g) is the weight of the sample before and after being treated.

$$C = \frac{m_2 - m_1}{m_1} \quad (3)$$

Results and discussion

Surface morphology and chemistry

The papers were fabricated by mussel-inspired surface coating technique, their micro-structures characterized as by SEM are shown in Fig. 2, and the elemental weights measured by EDS from Fig. 2B are listed in Table 1. The white pristine paper shows a three-dimensional structure consisting of microfibers

Table 1 Elemental weights of the samples characterized by EDS from SEM images in Fig. 2B

	Elements (wt%)			
Sample	C	O	N	Si
Paper	56.9	43.1	—	—
PDA/paper	67.2	25.0	7.8	—
PDMS–SiO_2/PDA/paper	17.5	38.9	0.4	43.2
PDMS–SiO_2/paper	30.7	41.0	—	28.3

Table 2 Thickness, porosity, tensile strength and elongation at break of the papers before and after surface coating

Sample	Thickness (μm)	Porosity (%)	Tensile strength (MPa)	Elongation at break (%)
Paper	265.4 ± 3.4	87.4 ± 1.3	7.8 ± 0.6	23.8 ± 2.3
PDA/paper	287.4 ± 3.6	81.2 ± 1.7	8.4 ± 0.5	26.3 ± 1.0
PDMS–SiO_2/PDA/paper	298.8 ± 5.1	77.0 ± 2.1	7.7 ± 0.8	27.5 ± 1.6
PDMS–SiO_2/paper	293.4 ± 7.4	69.2 ± 3.5	8.1 ± 0.7	28.9 ± 2.7

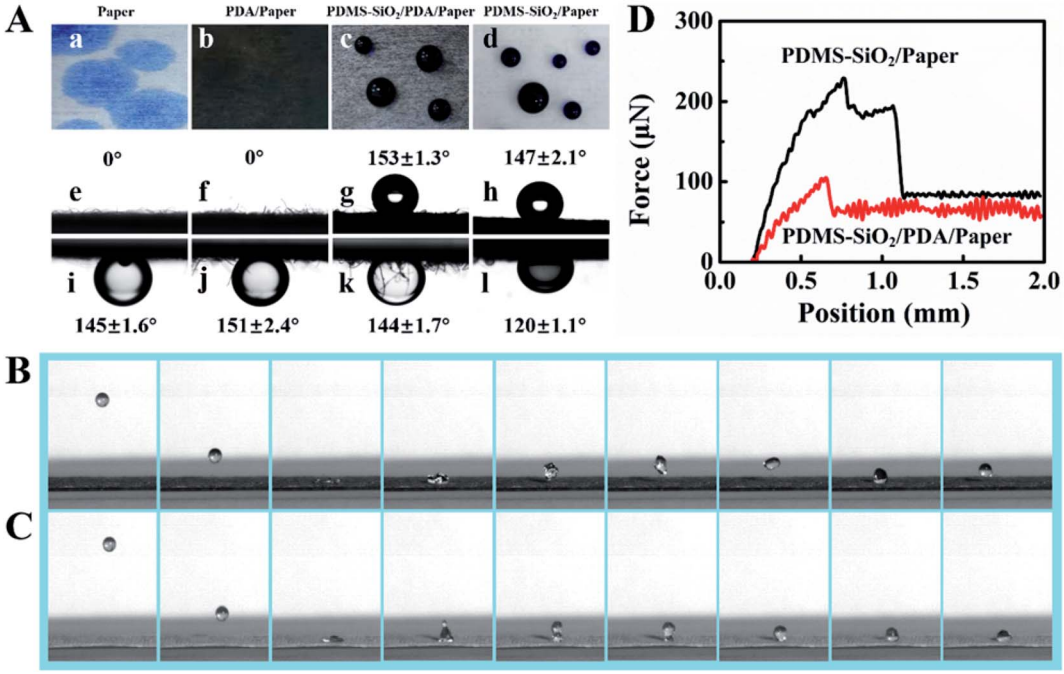

Fig. 3 (A) Digital pictures of the water droplets dyed by methylene blue on the papers (a to d), water contact angles in air (e to h), underwater oil (soybean oil) contact angles (i and g), underoil (trichloromethane) water contact angles (k and l) of the paper before and after modification. (B and C) Photographs of water droplets bouncing on PDMS–SiO_2/PDA/paper and PDMS–SiO_2/paper. (D) Water-adhesion forces on the sample surfaces.

with a diameter of 11.4 ± 0.3 μm. Only peaks of C and O are detected by EDS. After coating PDA for 12 h, the granules distribute loosely and randomly on the fibers, and the color of PDA/paper changes into dark brown. Three elements of C, O and N are simultaneously presented, and N accounts for 7.8 wt%. Upon being attached by PDMS and SiO_2 nanoparticles, PDMS–SiO_2 micro/nanoparticles overlapped densely around PDA particles, and the resultant PDMS–SiO_2/PDA/paper becomes light. In addition, seen from Table 1, new Si element appears and accounts for 43.2 wt%, while N can be neglected. It confirmed that PDMS–SiO_2 layer was successfully coated on PDA/paper. White PDMS–SiO_2/paper exhibits a significantly lower roughness, and the elements of C, O and Si were also detected. The results indicated that PDA particles play important role in development of a micro/nanoscale hierarchical structure on the fiber surface.[44,45] In addition, after surface coating, the thickness increases, the porosity decreases, tensile strength and elongation at break of the papers scarcely change (Table 2). Mussel-inspired surface modification technique is mild and facile.

Surface wettability

The contact angles of the paper before and after surface modification are shown in Fig. 3A. The water contact angles in air of paper (a and e) and PDA/paper (b and f) are about 0°, and their underwater oil (soybean oil) contact angles are 145 ± 1.6 (i) and 151 ± 2.4° (j), thus suggesting a superhydrophilic and underwater oleophobic properties. Upon modified by PDMS–SiO_2, tissue papers become hydrophobic (c and d). Compared with PDMS–SiO_2/paper, PDMS–SiO_2/PDA/paper is more hydrophobic with a water contact angle in air of ~153° (g) and an underoil (trichloromethane) water contact angle of ~144° (k). Furthermore, the bouncing behavior of water droplet on the hydrophobic surface was investigated. As shown in Fig. 3B, the water droplet rebounds on the superhydrophobic surface of PDMS–SiO_2/PDA/paper without wetting or even residual. While, the water droplet sticks to the surface of PDMS–SiO_2/paper and finally rest on the surface. The water-adhesion force of PDMS–SiO_2/paper (229.3 μN) is obviously larger than that of PDMS–SiO_2/PDA/paper (104.9 μN) (Fig. 3C). All the results illustrated

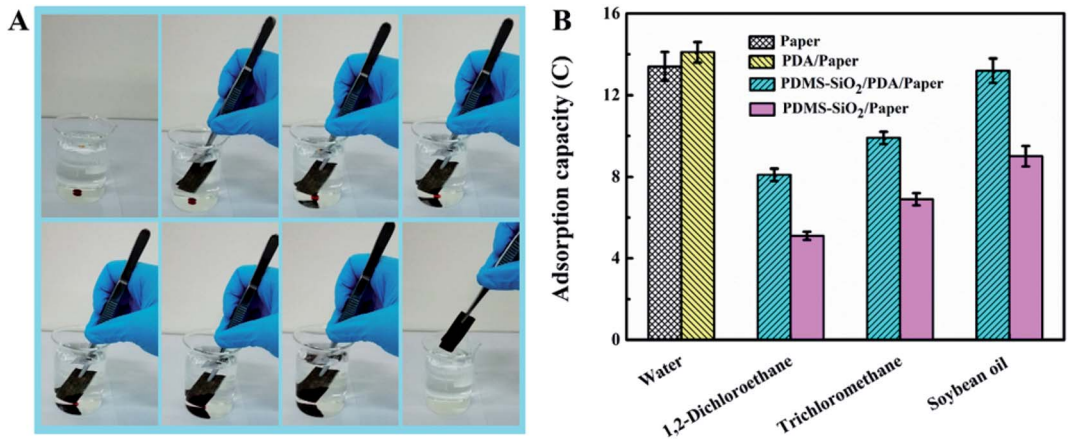

Fig. 4 (A) Photographs of the underwater oil (trichloromethane) capture and collection process by PDMS–SiO_2/PDA/paper. (B) Absorption capacity of the papers before and after surface coating for various liquids.

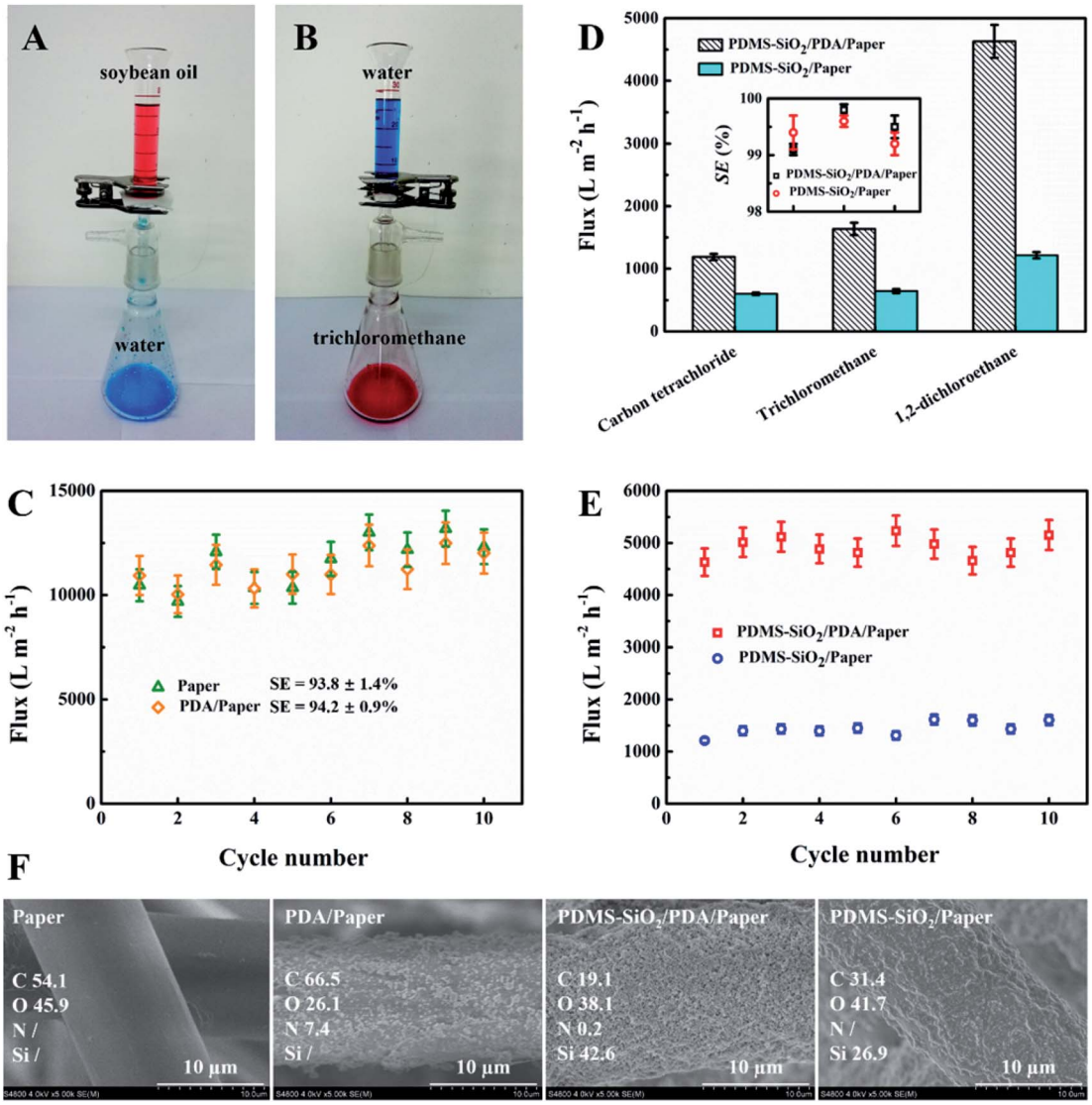

Fig. 5 (A) Photograph of soybean oil/water separation using paper. (B) Photograph of water/trichloromethane separation using PDMS–SiO_2/PDA/paper. (C) Water flux for soybean oil/water mixture. (D) Oil flux and separation efficiency for various oil/water mixtures. (E) The recycled separation flux of 1,2-dichloroethane/water mixture. (F) SEM images and elemental weights characterized by EDS of the samples after 10 cycles of reuse.

that the satisfactory superhydrophobic modification of the paper was achieved through the comprehensive utilization of PDA and PDMS–SiO_2, and liquids on the surface are in Cassie–Baxter state (low adhesive surface). This is because of a high surface roughness obtained by self-polymerization and deposition of dopamine as shown in Fig. 2. Moreover, it is attributed to more PDMS brushes and SiO_2 nanoparticles being generated.[30]

Absorption of liquid

Owing to open three-dimensional structure of the papers before and after modification, they showed great potential for the selective adsorption of liquid from water/oil mixture. As shown in Fig. 4A, PDMS–SiO_2/PDA/paper is able to adsorb trichloromethane (dyed with oil red O) immersing in water within 3 s. In addition, the adsorption capacity of the samples for various liquid was calculated and the results are shown in Fig. 4B. It is indicated that the adsorption capacity of water for paper is almost the same as that of PDA/paper, due to their similar micro-structure and hydrophilicity. Compared with PDMS–SiO_2/paper, PDMS–SiO_2/PDA/paper has a high absorption capacity for 1,2-dichloroethane, trichloromethane and soybean oil.

Oil/water separation

The separation performances of the paper before and after surface modification for different oil/water mixtures were investigated under gravity driving conditions. Upon dumping soybean oil/water into the apparatus, water quickly penetrates through the sample of paper due to it superhydrophilicity, while soybean oil is retained on the surface because of its under-water oleophobicity, as depicted in Fig. 5A. The corresponding water flux was more than 10 000 L m^{-2} h^{-1}, and the separation efficiency (SE) is 93.8 ± 1.4% (Fig. 5C). In addition, paper showed stable oil/water separation performance after 10 cycles of reuse. PDA/paper also can effectively separate soybean oil/water mixture. The separation treatment of immiscible heavy oil (carbon tetrachloride, trichloromethane, 1,2-dichloroethane)/water was similarly conducted by PDMS–SiO_2/PDA/paper and PDMS–SiO_2/paper. As shown in Fig. 5B, heavy oil penetrates through the sample due to its oleophilicity, while water is collected on the surface because of its under-oil hydrophobic properties. As summarized in Fig. 5D, compared with PDMS–SiO_2/paper, the corresponding oil fluxes of PDMS–SiO_2/PDA/paper are obviously larger, ascribing to higher porosity and under-oil hydrophobicity. The SE values of the samples for these

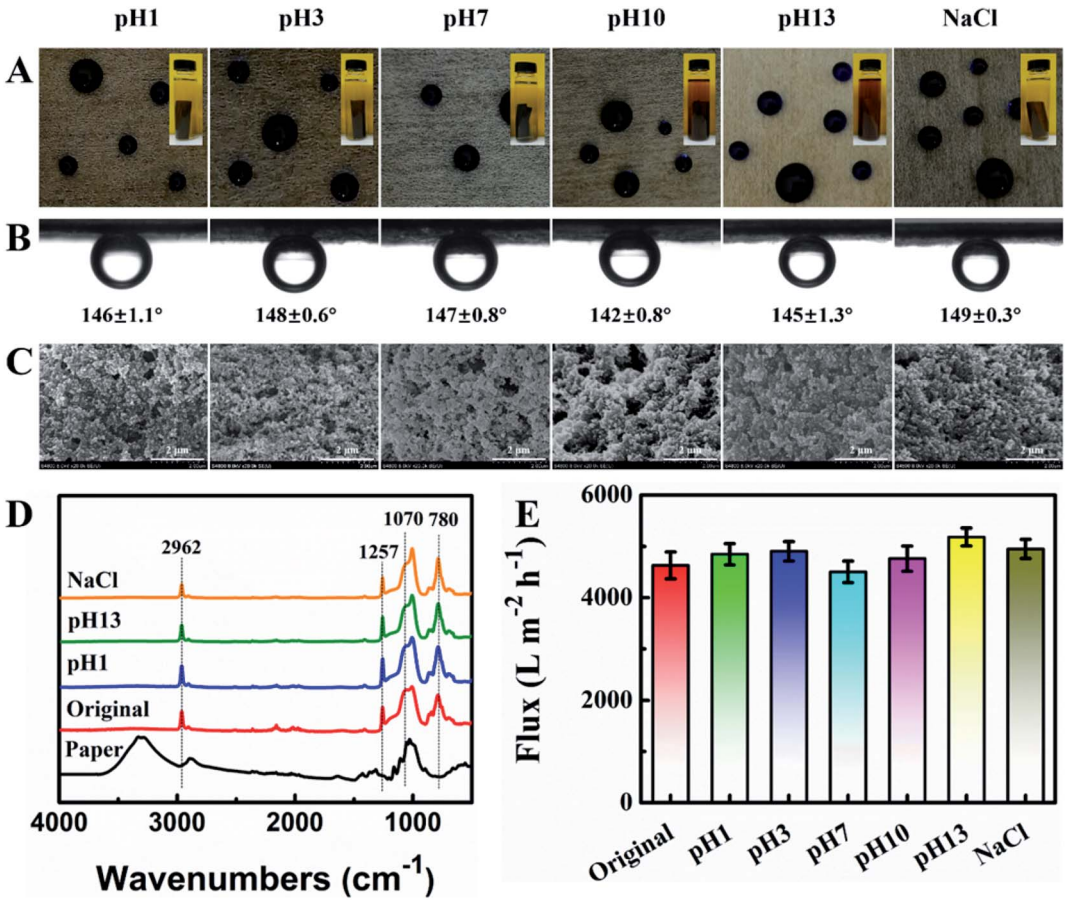

Fig. 6 (A) Digital pictures of the water droplets dyed by methylene blue, (B) underoil (trichloromethane) water contact angles, (C) SEM images, (D) ATR-FTIR spectra, and (E) oil fluxes for separation of 1,2-dichloroethane/water mixture of PDMS–SiO_2/PDA/paper after shaken in acidic (pH 1, pH 3), pure water (pH 7), alkaline (pH 10, pH 13) and salty (2 M NaCl) at 60 °C for 7 days. Insets in (A) corresponding photographs of the different aqueous solutions with PDMS–SiO_2/PDA/paper.

heavy oil/water mixtures were found to be higher than 99%, demonstrating almost complete separation processes. More important, after 10 cycles, oil fluxes of PDMS–SiO_2/PDA/paper and PDMS–SiO_2/paper are similar to the initial values respectively, suggesting the oil/water separation behavior of the samples is fully reversible. And the surface morphology and chemical composition of the samples after 10 cycles of reuse hardly change as shown in Fig. 5F. The results indicated that all the papers before and after modification showed stable oil–water separation performance and chemical stability.

Stability

The significant feature of the materials for efficient separation oil/water mixture is the stability and durability in acidic, alkaline and salty. In this test, the as-prepared hydrophobic PDMS–SiO_2/PDA/paper was first immersed in ethanol for 30 min, taken out and shaken in aqueous solutions at pH 1, 3, 7, 10, and 13, as well as aqueous solution of 2 M NaCl at 60 °C for continuous 7 days. Compared with the pristine PDMS–SiO_2/PDA/paper, the tensile strength and elongation at break of the washed samples in various solution changed barely. It was found that the solution color changes from colorless to brown, as pH value increases from 1 to 13, and the washed sample turns from dark drown to faint yellow (Fig. 6A). The strongly alkaline solution leads PDA disassembly or destacking.[33,46] The underoil (trichloromethane) water contact angle of the sample after washing is more than 140° (Fig. 6A). The multiscale structures of the washed samples are also observed in Fig. 6C. Fig. 6D shows the ATR-FTIR spectra of the samples. Compared with the pristine paper, all the spectra of the washed PDMS–SiO_2/PDA/paper exhibit the characteristic signals of Si–C bond (at 1257 and 780 cm^{-1}), Si–O–Si bond (at 1070 cm^{-1}), and C–H stretching vibration (at 2962 cm^{-1}),[30] suggesting the good stability of PDMS–SiO_2 layer on the PDA modified paper substrate. Seen from Fig. 6E, after immersion in the solution of pH 13, the flux of the modified papers washed under various solutions did not change much. All the results indicated that PDMS–SiO_2/PDA/paper exhibits good stability in acidic, alkaline and salty.

Conclusions

In summary, we have developed a simple strategy for fabricating superhydrophobic paper having the capacity to separate oil–water mixtures under gravity driving conditions. The nascent papers were coated with a PDA layer and then immersed in the mixtures of PDMS and hydrophobic-SiO_2 nanoparticles. It is shown that the micro/nanoscale hierarchical particles of PDMS–SiO_2/PDA covered on the porous substrate. The water droplets can rebound on the modified low energy surface without wetting or even residual. Upon dumping oil–water mixture into the surface, heavy oil quickly penetrates through the sample, while water is retained on the surface. The separation efficiency is larger than 99%. Furthermore, the modified paper shows excellent recyclability and stability in acidic, alkaline and salty. We believe that such a high-efficiency, low-cost and eco-friendly paper has great potential for the practical application in solve the oily wastewater.

Conflicts of interest

There are no conflicts to declare.

Acknowledgements

This work is supported by Zhejiang Baocheng Machine Science Technology Co., Ltd.

Notes and references

1 C. H. Lee, B. Tiwari, D. Zhang and Y. K. Yap, *Environ. Sci.: Nano*, 2017, **4**, 514–525.
2 X. Lin and J. Hong, *Adv. Funct. Mater.*, 2019, **6**, 1900126.
3 W. Ma, Q. Zhang, D. Hua, R. Xiong, J. Zhao, W. Rao, S. Huang, X. Zhan, F. Chen and C. Huang, *RSC Adv.*, 2016, **6**, 12868–12884.
4 B. S. Al-anzi and O. C. Siang, *RSC Adv.*, 2017, **7**, 20981–20994.
5 T. Krasian, W. Punyodom and P. Worajittiphon, *Chem. Eng. J.*, 2019, **369**, 563–575.
6 J. Gu, P. Xiao, P. Chen, L. Zhang, H. Wang, L. Dai, L. Song, Y. Huang, J. Zhang and T. Chen, *ACS Appl. Mater. Interfaces*, 2017, **9**, 5968–5973.
7 M. Peng, Y. Zhu, H. Li, K. He, G. Zeng, A. Chen, Z. Huang, T. Huang, L. Yuan and G. Chen, *Chem. Eng. J.*, 2019, **373**, 213–226.
8 Z. Chu, Y. Feng and S. Seeger, *Angew. Chem., Int. Ed. Engl.*, 2015, **54**, 2328–2338.
9 C. Ong, Y. Shi, J. Chang, F. Alduraiei, Z. Ahmed and P. Wang, *Ind. Eng. Chem. Res.*, 2019, **58**, 4838–4843.
10 G. Wang, Y. He, H. Wang, L. Zhang, Q. Yu, S. Peng, X. Wu, T. Ren, Z. Zeng and Q. Xue, *Green Chem.*, 2015, **17**, 3093–3099.
11 S. R. Chowdhury, A. Jha, U. Manna and K. S. S. Sarma, *RSC Adv.*, 2016, **6**, 26086–26095.
12 M. Padaki, R. Surya Murali, M. S. Abdullah, N. Misdan, A. Moslehyani, M. A. Kassim, N. Hilal and A. F. Ismail, *Desalination*, 2015, **357**, 197–207.
13 Y. Zhu, J. Wang, F. Zhang, S. Gao, A. Wang, W. Fang and J. Jin, *Adv. Funct. Mater.*, 2018, **28**, 1804121.
14 J.-B. Fan, Y. Song, S. Wang, J. Meng, G. Yang, X. Guo, L. Feng and L. Jiang, *Adv. Funct. Mater.*, 2015, **25**, 5368–5375.
15 M.-X. Hu, H.-M. Niu, X.-L. Chen and H.-B. Zhan, *Colloids Surf., A*, 2019, **564**, 142–151.
16 H.-M. Song, C. Chen, X.-X. Shui, H. Yang, L.-J. Zhu, Z.-X. Zeng and Q.-J. Xue, *J. Membr. Sci.*, 2019, **573**, 126–134.
17 Y. Chen, X. Li, M. J. Glasper, L. Liu, H.-J. Chung and J. A. Nychka, *RSC Adv.*, 2016, **6**, 92833–92838.
18 X. Chen, Y. Zhai, X. Han, H. Liu and Y. Hu, *Appl. Surf. Sci.*, 2019, **483**, 399–408.
19 L. Tie, J. Li, Z. Guo, Y. Liang and W. Liu, *Chem. Eng. J.*, 2019, **369**, 463–469.
20 F. L. Heale, M. Einhorn, K. Page, I. P. Parkin and C. J. Carmalt, *RSC Adv.*, 2019, **9**, 20332–20340.
21 Y. Cai, D. Chen, N. Li, Q. Xu, H. Li, J. He and J. Lu, *J. Membr. Sci.*, 2017, **543**, 10–17.

22 B. Cheng, Z. Li, Q. Li, J. Ju, W. Kang and M. Naebe, *J. Membr. Sci.*, 2017, **534**, 1–8.
23 R. K. Upadhyay, A. Dubey, P. R. Waghmare, R. Priyadarshini and S. S. Roy, *RSC Adv.*, 2016, **6**, 62760–62767.
24 X. Ou, X. Yang, J. Zheng and M. Liu, *ACS Sustainable Chem. Eng.*, 2019, **7**, 13379–13390.
25 Y. Liu, W. Tu, M. Chen, L. Ma, B. Yang, Q. Liang and Y. Chen, *Chem. Eng. J.*, 2018, **336**, 263–277.
26 Y. Jiang, J. Hou, J. Xu and B. Shan, *Carbon*, 2017, **115**, 477–485.
27 L. Li, B. Li, J. Dong and J. Zhang, *J. Mater. Chem. A*, 2016, **4**, 13677–13725.
28 H. Liu, Y. Wang, J. Huang, Z. Chen, G. Chen and Y. Lai, *Adv. Funct. Mater.*, 2018, **28**, 1707415.
29 C.-H. Xue, Y.-R. Li, J.-L. Hou, L. Zhang, J.-Z. Ma and S.-T. Jia, *J. Mater. Chem. A*, 2015, **3**, 10248–10253.
30 Y. Liu, X. Wang and S. Feng, *Adv. Funct. Mater.*, 2019, **29**, 1902488.
31 G. Wang, Z. Zeng, H. Wang, L. Zhang, X. Sun, Y. He, L. Li, X. Wu, T. Ren and Q. Xue, *ACS Appl. Mater. Interfaces*, 2015, **7**, 26184–26194.
32 H. Kang, B. Zhao, L. Li and J. Zhang, *J. Colloid Interface Sci.*, 2019, **544**, 257–265.
33 J. Jiang, L. Zhu, L. Zhu, H. Zhang, B. Zhu and Y. Xu, *ACS Appl. Mater. Interfaces*, 2013, **5**, 12895–12904.
34 J. Sedo, J. Saiz-Poseu, F. Busque and D. Ruiz-Molina, *Adv. Mater.*, 2013, **25**, 653–701.
35 J. Zhao, X. Zhao, Z. Jiang, Z. Li, X. Fan, J. Zhu, H. Wu, Y. Su, D. Yang, F. Pan and J. Shi, *Prog. Polym. Sci.*, 2014, **39**, 1668–1720.
36 H. Lee, S. M. Dellatore, W. M. Miller and P. B. Messersmith, *Science*, 2007, **318**, 426–430.
37 J. Jiang, P. Zhang, L. Zhu, B. Zhu and Y. Xu, *J. Mater. Chem. B*, 2015, **3**, 7698–7706.
38 H. C. Yang, J. K. Pi, K. J. Liao, H. Huang, Q. Y. Wu, X. J. Huang and Z. K. Xu, *ACS Appl. Mater. Interfaces*, 2014, **6**, 12566–12572.
39 S. Ryu, Y. Lee, J. W. Hwang, S. Hong, C. Kim, T. G. Park, H. Lee and S. H. Hong, *Adv. Mater.*, 2011, **23**, 1971–1975.
40 Y. Xie, Q. Huang, M. Liu, K. Wang, Q. Wan, F. Deng, L. Lu, X. Zhang and Y. Wei, *RSC Adv.*, 2015, **5**, 68430–68438.
41 H.-C. Yang, J. Luo, Y. Lv, P. Shen and Z.-K. Xu, *J. Membr. Sci.*, 2015, **483**, 42–59.
42 Y. Liu, K. Ai and L. Lu, *Chem. Rev.*, 2014, **114**, 5057–5115.
43 S. M. Kang, I. You, W. K. Cho, H. K. Shon, T. G. Lee, I. S. Choi, J. M. Karp and H. Lee, *Angew. Chem., Int. Ed. Engl.*, 2010, **49**, 9401–9404.
44 J. Hu, J. Zhu, C. Jiang, T. Guo, Q. Song and L. Xie, *Colloids Surf., A*, 2019, **577**, 429–439.
45 B. S. Y. B. Wang, X. X. Hu, B. Peng and Z. W. Deng, *Adv. Mater. Interfaces*, 2017, **4**, 1600727–1600738.
46 D. R. Dreyer, D. J. Miller, B. D. Freeman, D. R. Paul and C. W. Bielawski, *Langmuir*, 2012, **28**, 6428–6435.